Original Research Paper

Influence of earthquake input angle on seismic response of curved girder bridge

CrossMark

Yongjun Ni [a,b,*], Jiayu Chen [b,c], Hualiang Teng [a], Hui Jiang [b]

[a] Department of Civil and Environmental Engineering, University of Nevada-Las Vegas, Las Vegas 89119, USA
[b] School of Civil Engineering, Beijing Jiaotong University, Beijing 100044, China
[c] Central Research Institute of Building and Construction Co., Ltd., Beijing 100088, China

ARTICLE INFO

ABSTRACT

The maximum seismic response of curved bridge is significantly related to the input angle of designated earthquake. Owing to structure irregularities, bridge reactions result from the interaction between the moment and torsion forces. Based on the solving of the seismic response of structure excited by a one-way earthquake input, a uniform expression of the unfavorable angle of the earthquake input was derived, and the corresponding maximum response of structure was determined. Considering the orthotropic and skewed dual-directional earthquake input manners, the most unfavorable angles for the two cases were also derived, respectively. Furthermore, a series finite element models were built to analyze the multi-component seismic responses by examining an example of curved girder bridge considering the variation of curvature radius and the bearings arrangement. The seismic responses of the case bridges, were excited by earthquakes at different input angles, and were calculated and analyzed using a response spectrum method. The input angles of earthquake excitation were progressively increased. From the analysis and comparison based on the calculation results mentioned above, the most unfavorable angle of earthquake excitation corresponding to the maximum seismic response of the curved bridge could be determined. It was shown that the most unfavorable angles of earthquake input resulted from the different response combination methods were essentially coherent.

1. Introduction

Curved bridges have been extensively applied to the construction of roads and railways. As an important variation of the girder bridge, the curved bridge is playing a significant role in bridge engineering. Since the 1970s, engineers have observed numerous devastating earthquakes globally that have severely impacted a large number of curved bridges. One of the most destructive cases known by engineering

researchers was the San Fernando earthquake in 1971, which caused serious damage to a multi-span girder bridge spanning between two large grade-separated interchanges projects. Since then, the research on the seismic responses of curved bridges has been given increased attention in the field of bridge engineering. Tseng and Penzien (1975a, 1975b) published two articles on the analysis results of the nonlinear seismic response of continuous curved bridges under severe earthquake. Williams and Godden (1979) published their experimental results derived from shake table model of curved girder bridge that had collapsed in the San Fernando earthquake and the corresponding theoretical results of their finite element analysis. Kawashimak and Penzien (1979) established the mechanical model of expansion joints by considering collision and yielding phenomena, and studied the influences of expansion joints on the seismic response of curved bridges. Wilson and Button (1982) discussed the stress direction of the structure response excited by the multi-directional earthquake input, but their results proved to be in the later documents applied only to the situation of single-degree-of-freedom (SDOF) structure as of one-way input. Li et al. (1984) developed a curved coordinate system to study the seismic response of the curved bridge. Yuan et al. (1996) analyzed the linear and nonlinear response of a 9-span continuous curved bridge considering the wave passage effect. Based on the analysis of two curved bridge newly constructed, Qin et al. (1996) discussed the seismic performance respecting on the yielding and deformation of piers and the sliding and collision of the expansion joints. Zhu et al. (2000, 2002) discussed the principle input angle of the irregular bridges based on the SRSS combination method, pointed out that the maximum response of irregular bridge could be obtained by using response spectrum analysis inputted along the arbitrary two directions in plane. The factors such as the curvature and the type of the connecting of the pier and the beam were also analyzed. Zhang et al. (1999) and Fan et al. (2003) determined the most unfavorable input direction based on the yielding surface function theory. Applying the fiber element in piers, the sliding elements to simulate the bearings and the contacting elements to simulate the collision of the adjacent upper structures, Nie et al. (2004) evaluated the seismic performance of a curved bridge. Based on the detailed comparison analysis of the multiple calculating methods on the curved bridge, Gao and Zhou (2005) verified that the CQC3 (complete quadratic combination 3) method was the proper method for obtaining the maximum seismic response under the multiple-direction earthquake inputs. Relying on the multiple shaking table array tests of small scale curved girder bridge, Saad et al. (2012) and Wieser et al. (2012) analyzed the influence of indices such as beam curvatures, seat types, foundation areas, and isolation measures on the curved girder bridges, it was shown that the seismic response of curved bridges was significantly affected by the parameters mentioned above.

The newly issued *Caltrans Seismic Design Criteria* (2013) presents two methods to calculate the elastic earthquake response of curved bridges, namely that the maximum of the two cases is used for the bridge design; the response combination of the longitudinal direction and the transverse direction by CQC3 method. Whether the Caltrans method is suitable for the curved girder bridge is still a question worthy of verification because of the detailed construction difference in California, USA and China.

Owing to the difference in determining the most unfavorable input direction of curved bridge by different methods, the unfavorable input angle of earthquake ground motion is much needed in order to evaluate the seismic behavior of curved bridge more coherently.

2.   Theory of computation

2.1.   Single-direction earthquake acceleration input along a random direction in plane

Suppose an x–y coordinate system is to be adopted by the structure, as shown in Fig. 1(a). The single-direction earthquake acceleration $\ddot{a}_{1(t)}$ is inputted along a random direction ($0° < \alpha < 180°$) in the x–y plane.

The dynamic equilibrium equation of the structure is given as Eq. (1)

$$M\ddot{v}_{(t)} + C\dot{v}_{(t)} + Kv_{(t)} = -M\big[I_x\cos(\alpha) + I_y\sin(\alpha)\big]\ddot{a}_{1(t)} \tag{1}$$

where M, C and K are the mass matrix, damping matrix and stiffness matrix of the system, respectively, I_x and I_y are the unit column vectors along the coordinates x and y, respectively, $-MI_x\ddot{a}_{1(t)}$ and $-MI_y\ddot{a}_{1(t)}$ are the earthquake inertia forces excited by the single-direction earthquake acceleration $\ddot{a}_{1(t)}$ inputted along the x axis and y axis, respectively, α is the input angle anticlockwise from the x axis. Solving Eq. (1), we can get

$$v_{ij}^{\alpha} = \gamma_j^{\alpha} S_d(T_i, \xi_i)\phi_{ij} \tag{2}$$

where ϕ_{ij} is the element of the vibration mode vector for the j-th mode of the i-th mass point of the system, $S_d(T_i, \xi_i)$ is the displacement response spectrum calculated by Duhamel integral method for the period T_i and the damping ratio of the structure ξ_i, γ_j^{α} is the modal participation coefficient of the j-th modal mass of the system excited by the single-direction earthquake along angle α. It can be then calculated using Eq. (3)

$$\gamma_j^{\alpha} = \frac{\Phi_j^{\mathrm{T}} M\big[I_x\cos(\alpha) + I_y\sin(\alpha)\big]}{\Phi_j^{\mathrm{T}} M\Phi_j} = \gamma_j^x\cos(\alpha) + \gamma_j^y\sin(\alpha) \tag{3}$$

where Φ_j is the vibration mode matrix, and Φ_j^{T} is its transport matrix, γ_j^x and γ_j^y are the modal participation coefficients of the j-th modal mass of the system along the global coordinate of x and y axes, respectively.

Substituting the Eq. (3) into Eq. (2), we can get

$$v_{ij}^{\alpha} = \big[\gamma_j^x\cos(\alpha) + \gamma_j^y\sin(\alpha)\big]S_d(T_j, \xi_j)\phi_{ij} = v_{ij}^x\cos(\alpha) + v_{ij}^y\sin(\alpha) \tag{4}$$

where v_{ij}^x and v_{ij}^y are the relative displacements for the j-th mode and the i-th mass point of the system under the single-direction earthquake acceleration $\ddot{a}_{1(t)}$ along the global coordinate of x and y axes, respectively. Similarly, we can get

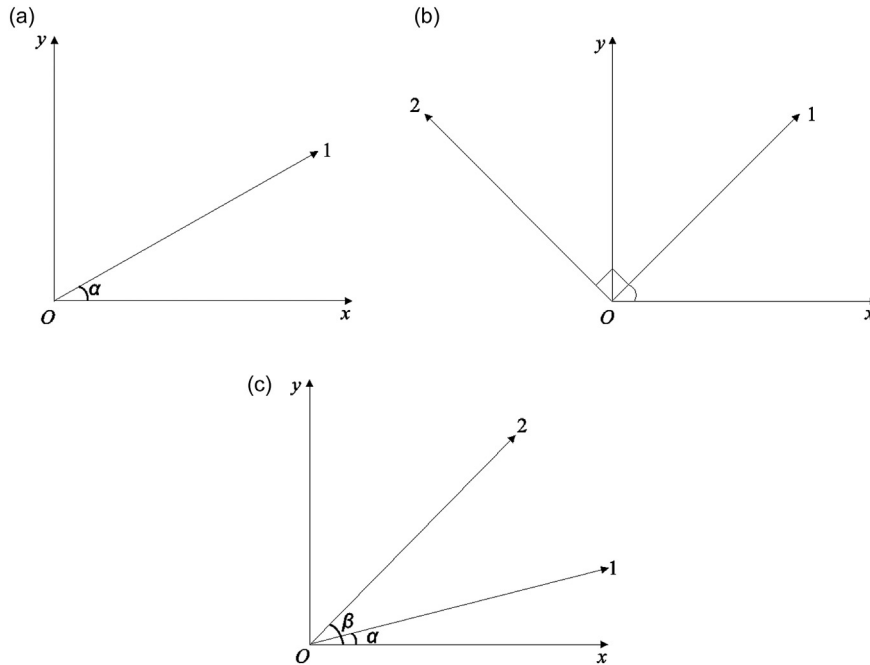$$R_{ij}^{\alpha} = R_{ij}^x\cos(\alpha) + R_{ij}^y\sin(\alpha) \tag{5}$$

Fig. 1 — Earthquake acceleration input angle. (a) Single-direction input. (b) Orthotropic dual-direction inputs. (c) Skewed dual-direction inputs.

where R_{ij}^α is the earthquake response (such as the bending moment, shearing force, deformation etc.) for the j-th mode and the i-th mass point under the single-direction earthquake along a random included angle α with x axis, R_{ij}^x and R_{ij}^y are the responses for the j-th mode and the i-th mass point along the global coordinate of x and y axes, respectively.

When the natural vibration property of the structure is controlled by the predominant mode, then the earthquake response R_i^α as the input angle α is

$$R_i^\alpha = R_i^x \cos(\alpha) + R_i^y \sin(\alpha) \tag{6}$$

where R_i^x and R_i^y are the responses for the i-th mass point of the system under the single-direction earthquake along x and y axes, respectively. From Eq. (6), taking

$$\alpha = \arctan\left(\frac{R_1^y}{R_1^x}\right) \tag{7}$$

we can get the maximum value $R_{i\max}^\alpha$ of R_i^α by

$$R_{i\max}^\alpha = \sqrt{\left(R_i^x\right)^2 + \left(R_i^y\right)^2} \tag{8}$$

When the related coefficient of each mode of the structure is smaller, we can adopt the SRSS method to combine the response of each mode. Then, we can get

$$R_i^\alpha = \sqrt{\sum_{j=1}^n \left(R_{ij}^\alpha\right)^2} = \sqrt{\left(R_i^x\right)^2 \cos^2\alpha + \left(R_i^y\right)^2 \sin^2\alpha + \sum_{j=1}^n R_{ij}^x R_{ij}^y \sin(2\alpha)} \tag{9}$$

where $R_i^x = \sqrt{\sum_{j=1}^n \left(R_{ij}^x\right)^2}$ and $R_i^y = \sqrt{\sum_{j=1}^n \left(R_{ij}^y\right)^2}$ are the responses for the i-th mass point under the single-direction earthquake along the global coordinate x and y axes, respectively, and combined using the SRSS method.

Both sides of Eq. (9) can been squared, then its uniform formula can be described as

$$y^2 = A\cos^2\alpha + B\sin^2\alpha + C\sin(2\alpha) \tag{10}$$

where $A = (R_i^x)^2$, $B = (R_i^y)^2$ and $C = \sum_{j=1}^n R_{ij}^x R_{ij}^y$.

The condition for y^2 to reach its maximum $y_{\max}^2$ is that the derivative of the right part of Eq. (10) is equal to zero, we can get the uniform calculating formulas of the most unfavorable angle of the earthquake input and the maximum response Eqs. (11) and (12)

$$\alpha = \frac{1}{2}\arctan\left(\frac{2C}{A-B}\right) \tag{11}$$

$$y_{\max}^2 = \frac{A+B}{2} \pm \sqrt{\left(\frac{A-B}{2}\right)^2 + C^2} \tag{12}$$

Taking

$$\alpha = \frac{1}{2}\arctan\left[\frac{2\sum_{j=1}^n R_{ij}^x R_{ij}^y}{\left(R_i^x\right)^2 - \left(R_i^y\right)^2}\right] \tag{13}$$

we can get the maximum value $R_{i\max}^\alpha$ of R_i^α by

$$\left(R_{i\max}^\alpha\right)^2 = \frac{\left(R_i^x\right)^2 + \left(R_i^y\right)^2}{2} \pm \sqrt{\left[\frac{\left(R_i^x\right)^2 - \left(R_i^y\right)^2}{2}\right]^2 + \left(\sum_{j=1}^n R_{ij}^x R_{ij}^y\right)^4} \tag{14}$$

When the related coefficient of each mode of the structure cannot be neglected, we can adopt the CQC method to combine the response of each mode, and arrive at

$$R_i^\alpha = \sqrt{\sum_{j=1}^{n} \sum_{k=1}^{n} \rho_{jk} R_{ij}^\alpha R_{ik}^\alpha}$$

$$= \sqrt{\left(R_i^x\right)^2 \cos^2\alpha + \left(R_i^y\right)^2 \sin^2\alpha + \sum_{j=1}^{n} \sum_{k=1}^{n} \rho_{jk} R_{ij}^x R_{ik}^y \sin(2\alpha)} \quad (15)$$

where ρ_{jk} is the related coefficient between the j-th mode and the k-th mode,
$R_i^x = \sqrt{\sum_{j=1}^{n} \sum_{k=1}^{n} \rho_{jk} R_{ij}^x R_{ik}^x}$ and $R_i^y = \sqrt{\sum_{j=1}^{n} \sum_{k=1}^{n} \rho_{jk} R_{ij}^y R_{ik}^y}$ are the responses for the i-th mass point of the system under the single-direction earthquake along the global coordinate of x and y axes, respectively, and combined using the CQC method. Taking

$$\alpha = \frac{1}{2}\arctan\left[\frac{2\sum_{j=1}^{n} \rho_{jk} R_{ij}^x R_{ij}^y}{\left(R_i^x\right)^2 - \left(R_i^y\right)^2}\right] \quad (16)$$

we can get the maximum value R_{imax}^α of R_i^α by

$$\left(R_{imax}^\alpha\right)^2 = \frac{\left(R_i^x\right)^2 + \left(R_i^y\right)^2}{2} \pm \sqrt{\left[\frac{\left(R_i^x\right)^2 - \left(R_i^y\right)^2}{2}\right]^2 + \left(\sum_{j=1}^{n} \rho_{jk} R_{ij}^x R_{ij}^y\right)^4} \quad (17)$$

2.2. Orthotropic dual direction earthquakes input along a random direction in plane

As shown in Fig. 1(b), the orthotropic double-direction earthquake accelerations $\ddot{a}_{1(t)}$, $\ddot{a}_{2(t)}$, inputted along a random

where R_i^α is the response of the i-th mass point of the system under the orthotropic double-direction earthquakes along the directions shown in Fig. 1(b), each of $R_i^{1\alpha}$, R_i^{1x} and R_i^{1y} stands for one of the orthotropic double-direction earthquake accelerations $\ddot{a}_{1(t)}$ inputted along the direction shown in Fig. 1(b). Likewise, the meanings of $R_i^{2\alpha}$, R_i^{2x}, and R_i^{2y} are similar to that of $R_i^{1\alpha}$, R_i^{1x} and R_i^{1y}.

Supposing that the displacement response spectrum of dual-direction has the same conversion, and their relation is as Eq. (19)

$$S_2(T_i, \xi_i) = \lambda S_1(T_i, \xi_i) \quad (19)$$

where λ is defined as the percentage coefficient to adjust the peak ground acceleration (PGA) of the designated earthquake along the different input direction, $\lambda < 1$.

Eq. (18) can be derived as Eq. (20)

$$R_i^\alpha = \sqrt{\left[\left(R_i^{1x}\right)^2 + \lambda^2 \left(R_i^{1y}\right)^2\right]\cos^2\alpha + \left[\left(R_i^{1y}\right)^2 + \lambda^2 \left(R_i^{1x}\right)^2\right]\sin^2\alpha + \left[\left(1 - \lambda^2\right)R_i^{1x}R_i^{1y}\right]\sin(2\alpha)} \quad (20)$$

Taking $\alpha = \frac{1}{2}\arctan\left[\frac{2R_i^{1x}R_i^{1y}}{\left(R_i^{1x}\right)^2 - \left(R_i^{1y}\right)^2}\right]$, we can get the maximum value R_{imax}^α of R_i^α as Eq. (21)

$$\left(R_{imax}^\alpha\right)^2 = \frac{\left(R_i^x\right)^2 + \left(R_i^y\right)^2}{2} \pm \sqrt{\left[\frac{\left(R_i^x\right)^2 - \left(R_i^y\right)^2}{2}\right]^2 + \left(R_i^x R_i^y\right)^4} \quad (21)$$

When the related coefficient of each mode of the structure is smaller, and Eq. (19) is satisfied, we can adopt the SRSS method to combine the seismic responses of each mode for two directions, in a similar process to reach

$$R_i^\alpha = \sqrt{\left[\left(R_i^{1x}\right)^2 + \lambda^2 \left(R_i^{1y}\right)^2\right]\cos^2\alpha + \left[\left(R_i^{1y}\right)^2 + \lambda^2 \left(R_i^{1x}\right)^2\right]\sin^2\alpha + \left[\left(1 - \lambda^2\right)\left(\sum_{j=1}^{n} \sum_{k=1}^{n} R_{ij}^{1x} R_{ik}^{1y}\right)\right]\sin(2\alpha)} \quad (22)$$

direction α ($0° < \alpha < 180°$) in plane are perpendicular to each other.

Supposing that the structure response is controlled by the predominant mode, we can adopt the SRSS method to combine the seismic responses of two directions, obtaining

Taking $\alpha = \frac{1}{2}\arctan\left[\frac{2\sum_{j=1}^{n}\sum_{k=1}^{n} R_{ij}^{1x} R_{ij}^{1y}}{\left(R_i^{1x}\right)^2 - \left(R_i^{1y}\right)^2}\right]$, we can get the maximum value R_{imax}^a of R_i^α as

$$R_i^\alpha = \sqrt{\left(R_i^{1\alpha}\right)^2 + \left(R_i^{2\alpha}\right)^2} = \sqrt{\left[\left(R_i^{1x}\right)^2 + \left(R_i^{2y}\right)^2\right]\cos^2\alpha + \left[\left(R_i^{1y}\right)^2 + \left(R_i^{2x}\right)^2\right]\sin^2\alpha + \left(R_i^{1x}R_i^{1y} - R_i^{2x}R_i^{2y}\right)\sin(2\alpha)} \quad (18)$$

$$\left(R_{imax}^{\alpha}\right)^2 = \frac{\left(R_i^x\right)^2 + \left(R_i^y\right)^2}{2} \pm \sqrt{\left[\frac{\left(R_i^x\right)^2 - \left(R_i^y\right)^2}{2}\right]^2 + \left(R_i^x R_i^y\right)^4}$$

which has the same expression as Eq. (21).

When the related coefficient of each mode of the structure cannot be neglected, we can adopt the CQC method to combine the seismic response of each mode and use the SRSS method to combine the two directions to get

$$R_i^{\alpha} = \sqrt{\left[\left(R_i^{1x}\right)^2 + \lambda^2\left(R_i^{1y}\right)^2\right]\cos^2\alpha + \left[\left(R_i^{1y}\right)^2 + \lambda^2\left(R_i^{1x}\right)^2\right]\sin^2\alpha + \left[(1-\lambda^2)\left(\sum_{j=1}^{n}\sum_{k=1}^{n}\rho_{jk}R_{ij}^{1x}R_{ik}^{1y}\right)\right]\sin(2\alpha)} \tag{23}$$

Taking $\alpha = \frac{1}{2}\arctan\left[\frac{2\sum_{j=1}^{n}\rho_{jk}R_{ij}^x R_{ij}^y}{\left(R_i^x\right)^2 - \left(R_i^y\right)^2}\right]$, we can get the maximum value R_{imax}^{a} of R_i^{a} as $\left(R_{imax}^{\alpha}\right)^2 = \frac{\left(R_i^x\right)^2 + \left(R_i^y\right)^2}{2} \pm$ $\sqrt{\left[\frac{\left(R_i^x\right)^2 - \left(R_i^y\right)^2}{2}\right]^2 + \left(R_i^x R_i^y\right)^4}$, which has the same expression as Eq. (21).

2.3. Skewed dual-direction earthquakes inputted along a random direction in plane

For some special mountainous sites, the earthquakes maybe inputted as the skewed angle as shown in Fig. 1(c), it could be realized and verified by the investigation of 2008 Wenchuan Earthquake in China (Zhou, 2010). The skewed dual-direction earthquake accelerations $\ddot{a}_{1(t)}$, $\ddot{a}_{2(t)}$, are inputted along a random direction α, β ($0° < \alpha$, $\beta < 180°$) in the same plane, respectively.

Adopting the SRSS method to combine the seismic responses of the two directions, we can get

$$R_i^{\alpha\beta} = \sqrt{\left(R_i^{\alpha}\right)^2 + \left(R_i^{\beta}\right)^2} \tag{24}$$

Adopting the percentage method to combine the two directions, we can get

$$R_i^{\alpha\beta} = R_i^{\alpha} + \lambda R_i^{\beta} \tag{25}$$

where $R_i^{\alpha\beta}$ is the response of the i-th mass point of the system excited by the skewed dual-direction earthquakes inputted along the direction as shown in Fig. 1(c), R_i^{α}, R_i^{β} are the responses for the i-th mass point of the system under the skewed earthquakes as shown in Fig. 1(c).

Using the similar procedures like Eqs. (10)–(12), the most unfavorable angle of the earthquake input α and the maximum value R_{imax}^{α} of R_i^{α}, a similar expression can be obtained.

3. Numeric example of the curved bridge

3.1. Introduction of case bridge

We now examine a three-span continuous curved bridge (Fig. 2) with the span of 73 m + 130 m + 73 m. The piers of the bridge with piles foundation are single columns with rectangular sections (13 m × 3 m), with pier heights varied as 9, 10, 11 and 12 m. The main beam is a single-box double-cell girder, and the heights of the top beam and mid-span beam are 8.0 and 3.5 m, respectively. The height of the beam changes along the span direction in accordance with a second-degree parabola. All bearings are pot rubber bearings, allocated as Fig. 3, in which, DX means the bearing can only be moved along longitudinal direction or transverse directions; SX indicates the bearing can be moved both along the longitudinal and transverse directions; GD implies that the bearing is fixed. The stiffness of seating is taken as 12.5 × 10⁶ N/m. The concrete strength for the box girder and the piers are C50 and C40, respectively. The bridge is located on soft site (classified as
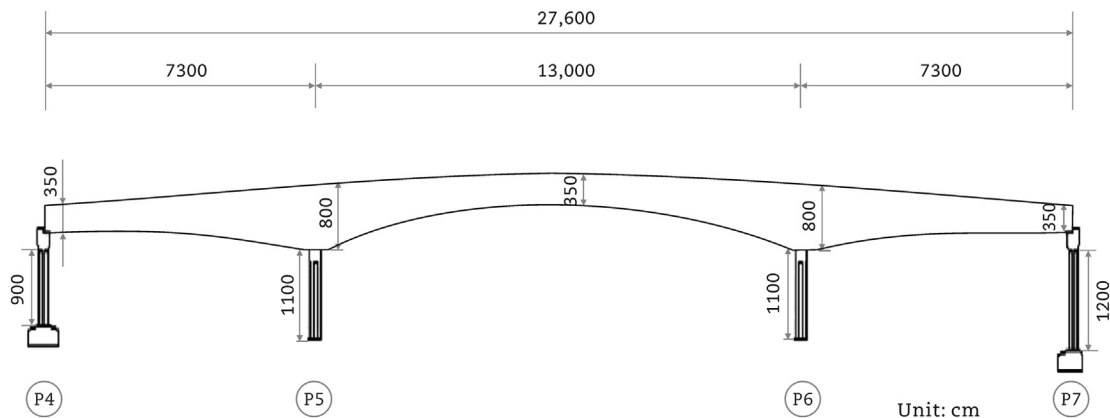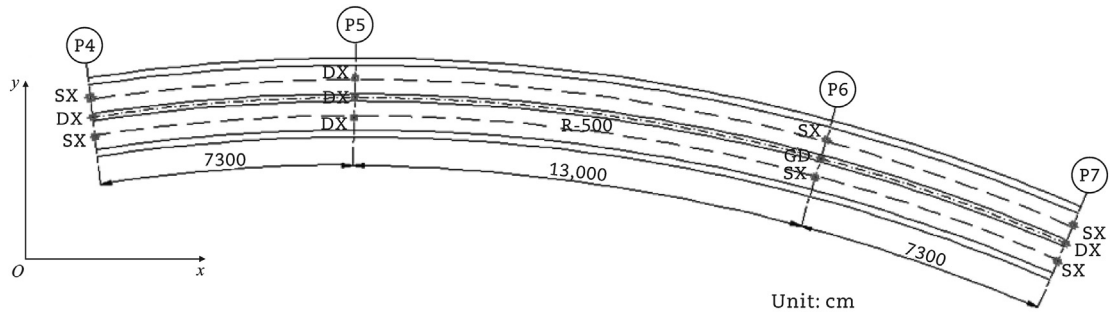

Fig. 2 − Elevation of curved girder bridge.

Fig. 3 – Plane allocation of curved girder bridge.

Site IV). Its design fortification intensity of earthquake is 8 (namely the peak ground acceleration of the horizontal design earthquake is 0.2g). Two types of bearing arrangement were considered as seen in Fig. 4. Fig. 4(a) means that the bearings are considered as the ideal sliding or fixed bearings. Fig. 4(b) indicates that all the bearings are considered as their actual stiffness.

The soil-structure interaction was neglected. The modal damping ratio of 5% was adopted.

Modal analysis was carried out to choose the top 20 modes for the response spectrum analysis. The maximum of the response spectrum was determined as Eq. (26) according to Guidelines for Seismic Design of Highway Bridges (2008).

$$S_{max} = 2.25C_iC_sC_dA \tag{26}$$

where C_i is the importance coefficient, 0.5 for E1 earthquake and 1.7 for E2 earthquake, C_s is the site coefficient, 1.0 for site IV, C_d is the damping adjustment coefficient, 1.0 for damping ratio of 5%, A is the peak ground acceleration of the horizontal design earthquake, 0.2g for the design fortification intensity of earthquake. In this paper, only E1 earthquake was considered.

3.2.   Single-direction earthquake inputted along any direction in plane

The case curved bridges (curvature radius are varied as 75, 175, 275 m and infinity (namely a direct-line layout bridge)) were excited by a series of one-way earthquake spectra along a varying angle (the angle increment is 3°) of the x axis within the range of 0°−180°. The global coordinate of x and y
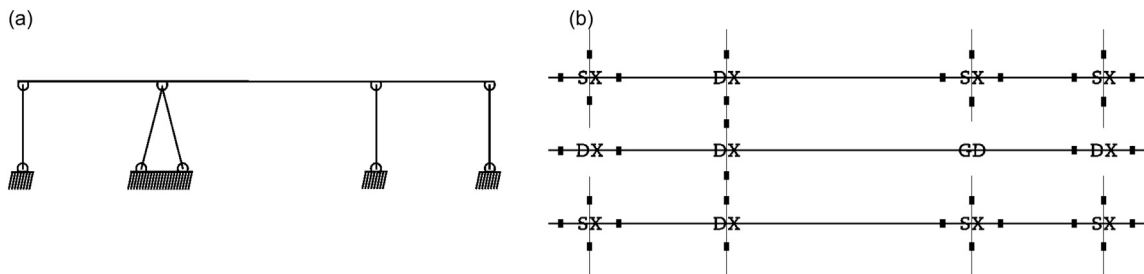

Fig. 4 – Two types of bearing arrangement. (a) Idealized bearing arrangement of continuous bridge. (b) Actual bearing arrangement.
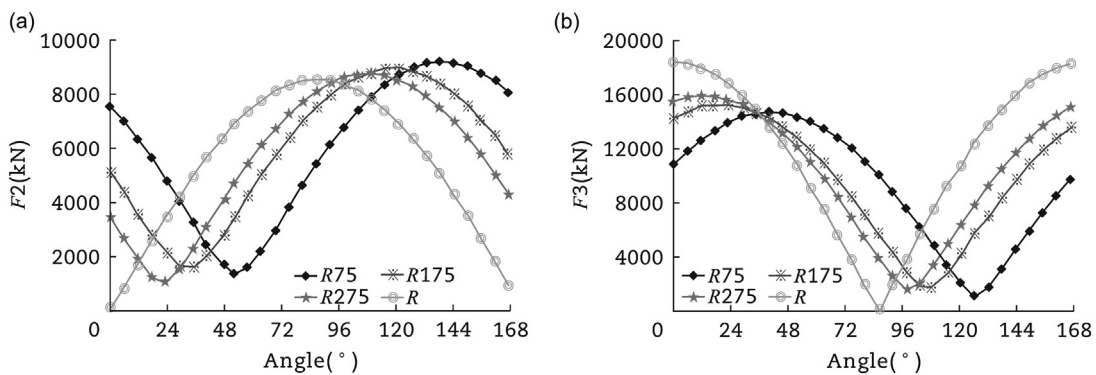

Fig. 5 – Base shearing forces of P5 for bearing arrangement as Fig. 4(a). (a) Base shearing forces along radial direction. (b) Base shearing forces along tangential direction.
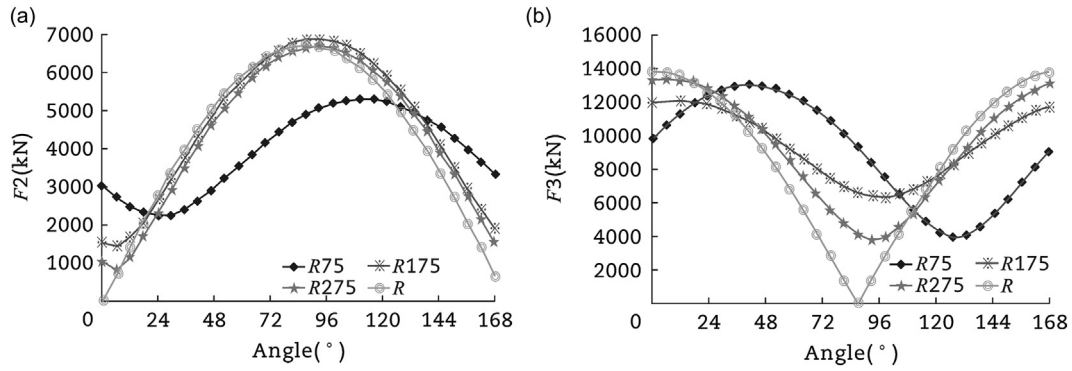
Fig. 6 — Base shearing forces of P5 for bearing arrangement as Fig. 4(b). (a) Base shearing forces along radial direction. (b) Base shearing forces along tangential direction.

axes were defined as the direction along the chord connection of the center abutments and its perpendicular direction shown.

The seismic responses were combined using the CQC method. The base shearing forces for all piers along the longitudinal and transverse direction were calculated. For conciseness, only the responses for P5 were listed from Figs. 5—8. The symbols R75, R175, R275 and R representing the curvature radius of the bridge are 75, 175, 275 m and infinity, respectively. F2 and F3 are the base shearing forces of piers along the radial and tangential direction in kN, respectively. M2 and M3 indicates the bending moments of piers around the radial and tangential directions in kN m, respectively.

Under the condition of the bearing arranged as Fig. 4(a), it can be seen from Figs. 5—7 that the base shearing forces and bending moments are varied as a trigonometric function rule with the incremental input angle. The phase angles of the trigonometric function are gradually increased while their wave lengths decreased with the reduction of the curvature radius of the bridge. Most of the response parameters but F2 show the gradually reduced tendency with the reduction of the curvature radius of the bridge.

It can be seen from Figs. 5—8 that all the responses in case of the bearings arranged as Fig. 4(b) are much less than those from Fig. 4(a). The amplitudes of the parameters F3 and M2 are greatly influenced by the bearings arrangement. For the parameters F2 and M3, not only their amplitudes are greatly influenced by the bearings arrangement, but also their varying rules with the curvature radius variation.

Considering the influences of the curvature radius of the bridge and the bearings arrangement on the seismic response of the curved bridge, the general varying tendency of the pier responses is shown in Table 1, in which the symbols "↑", "↓" and "≈" are used to describe the progressive increase, the progressive decrease and almost no change, respectively. The symbols ①, ②, ③ and ④ designate the amplitude, phase angle, wave length and functional value of the triangular function, respectively. And the symbol "★" means the maximum of the response for the pier in the cases mentioned above. R designates the curvature radius, "(a)" and "(b)" mean the bearing arrangements as Fig. 4(a) and (b), respectively.

3.3. Dual-directional earthquakes inputted along two directions in plane

For brevity, the curvature radius of the curved bridge was fixed to 500 m, and the bearings were arranged as Fig. 4(b). According to the calculating procedures above, considering the assumption of Eq. (19), the seismic responses under the dual-directional earthquakes were obtained using the SRSS and the percentage combination methods according to Eqs. (24) and (25), respectively. The orthogonal and skewed bi-
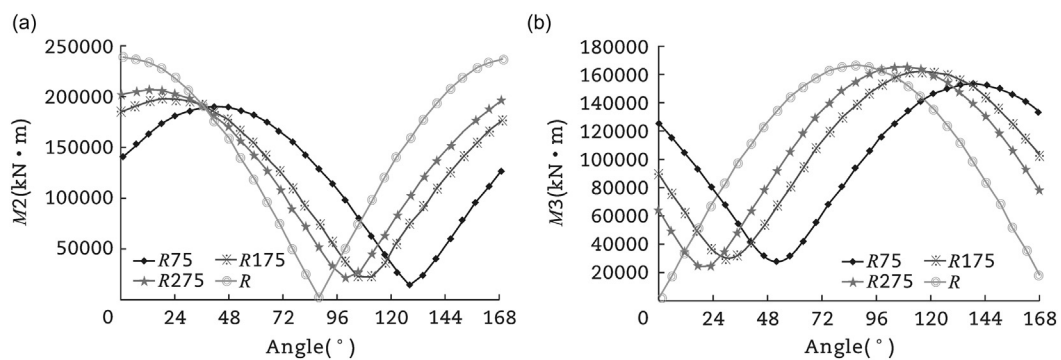

Fig. 7 — Bending moments of P5 for bearing arrangement as Fig. 4(a). (a) Bending moments around radial direction. (b) Bending moments around tangential direction.
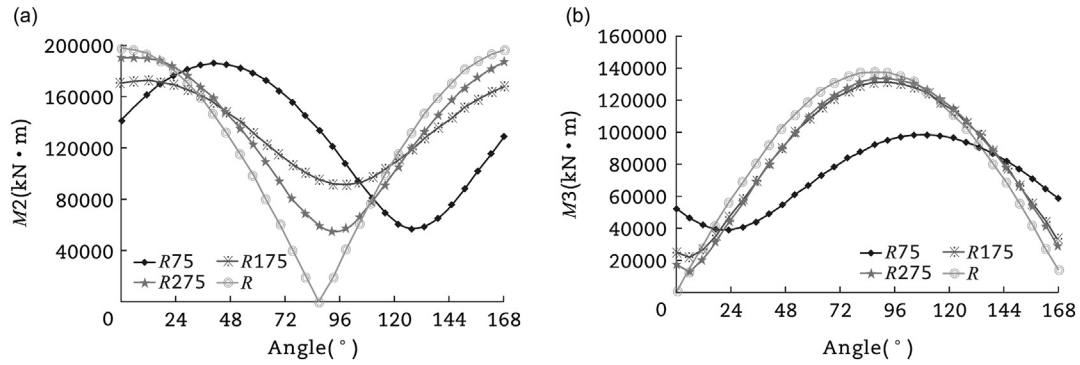
Fig. 8 – Bending moments of P5 for bearing arrangement as Fig. 4(b). (a) Bending moments around radial direction. (b) Bending moments around tangential direction.

direction earthquake inputs were included in the combination procedures. In this paper, only the base shearing forces for P4 are illustrated in Fig. 9.

It can be seen from Fig. 9 that the results from the two combination methods are significantly differed. The results

from the SRSS combination method are much greatly than those from the percentage method. The rationality of the calculating results should be verified by the results from the time history analysis. But the varying tendency from the two methods are essentially same. The former response can

Table 1 – Summary of varying tendencies of pier responses for curved bridge.

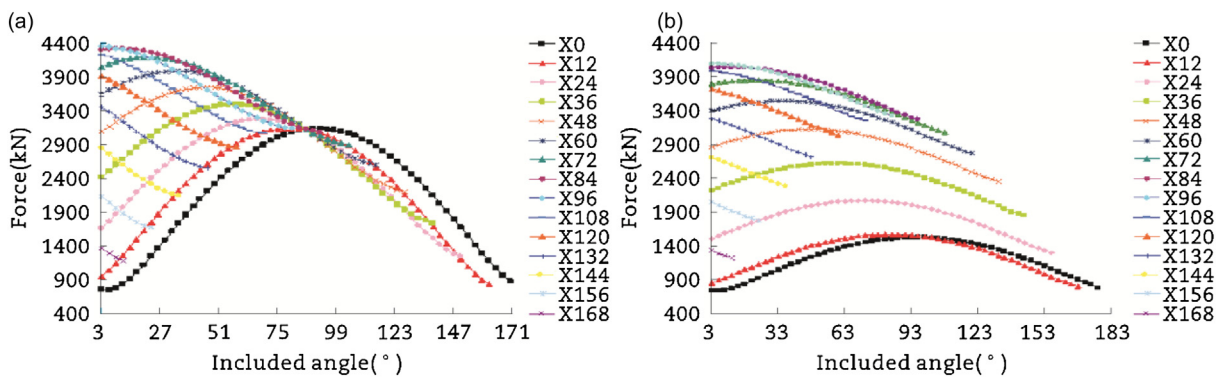| Pier no.	Influential factor	Variable	F2 (a)	F2 (b)	F3 (a)	F3 (b)	M2 (a)	M2 (b)	M3 (a)	M3 (b)
P4	R↓	①	≈	↓	≈	≈	≈	≈	↓	↓
		②	↑	↓	↑	↑	↑	↑	↑	↓
		③	↓	↓	≈	≈	≈	≈	↓	↓
	(a)→(b)	④	↑		≈		≈		↑	
P5	R↓	①	≈	≈	↓	↓	↓	↓	≈	≈
		②	↑	≈	↑	↑	↑	↑	↑	≈
		③	↓	↓	↓	↓	↓	↓	↓	↓
	(a)→(b)	④	↓		↓		↓		↓	
P6	R↓	①	↓	≈★	↑	↓★	↑	↓★	↓	↓★
		②	↓	↓	↓	↓	↓	↓	↓	↓
		③	↓	↓	↓	↓	↓	↓	↓	↓
	(a)→(b)	④	↑		↑		↑		↑	
P7	R↓	①	↓	↓	≈	≈	≈	≈	↓	↓
		②	↓	↓	↓	↓	↓	↓	≈	↓
		③	↓	↓	≈	≈	≈	≈	↓	↓
	(a)→(b)	④	↑		≈		≈		↑	

Fig. 9 – Base shearing forces of P4 excited by bi-directional response spectra along radial direction based on bearing arrangement as Fig. 4(b). (a) SRSS combination method. (b) Percentage combination method.
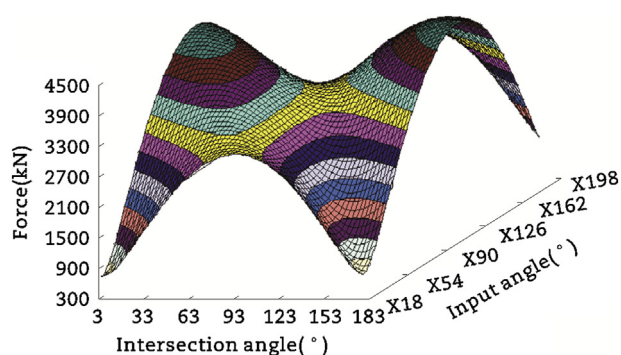
Fig. 10 – Radial shearing forces of P4 excited by bi-directional response spectra.

provide a conservative result for the seismic design of a curved bridge.

For further understand of the varying rule from the combination of the bi-directional responses, the results of Fig. 9(a) was changed to drawn as a three dimension chart as Fig. 10. In Fig. 10, the coordinate axis with X18, …, represents the input angle of the response spectrum; the horizontal axis indicates the intersection angle from the former axis. The vertical axis means the base shearing forces of P4 along the radial direction (in kN). The unfavorable angle for the designated response parameter under the condition of the dual-directional earthquake input can be easily determined.

4. Conclusions

(1) Under the reaction of single response spectrum, the seismic responses of the piers vary as a trigonometric tendency with respect to changes of the input angle, and the maximum response of an individual pier is far higher than the rest of the piers with respect to the reaction amount.

(2) The maximum response of each pier comes out at different angles, even for the same pier the maximum of differency appears from different angle. The application of the theoretical formula reduces the workload of statistics to a large extent, and makes it is more convenient to evaluate the most unfavorable input angles.

(3) The varying tendency results from the SRSS or percentage combination method tend to be similar. The results from the SRSS combination method can provide a conservative evaluation for the seismic design of curved bridge.

Acknowledgments

REFERENCES

Fan, L.C., Nie, L.Y., Li, J.Z., 2003. Discussion on standard of critical angle of seismic wave in seismic analysis of complicated structures. Journal of Tongji University: Natural Science 31 (6), 631–636.

Gao, X.A., Zhou, X.Y., 2005. Dynamic analysis method of the curved bridge under multi-component. Special Structures 22 (1), 56–60.

Kawashimak, K., Penzien, J., 1979. Theoretical and experimental dynamic behavior of a curved model bridge structure. Earthquake Engineering and Structural Dynamics 7 (2), 129–145.

Li, G.H., Shi, D., Heins, C.P., 1984. The finite element method of the seismic analysis of the curved bridge. Journal of Tongji University: Natural Science 23 (1), 1–21.

Nie, L.Y., Li, J.Z., Hu, S.D., et al., 2004. Nonlinear analysis and seismic estimation on curved beam bridge. Journal of Tongji University: Natural Science 32 (10), 1360–1364.

Qin, Q., Zhang, W., Luo, L., 1996. Seismic evaluation of overcrossing bridges using inelastic response analysis. China Civil Engineering Journal 29 (4), 3–10.

Saad, A.S., Sanders, D.H., Buckle, L.G., 2012. Effect of rocking foundations on seismic behavior of horizontally curved bridges with different degree of curvatures. In: Proceedings of 15th World Conference on Earthquake Engineering, Lisbon, 2012.

Tseng, W.S., Penzien, J., 1975a. Seismic analysis of long multiple-span highway bridges. Earthquake Engineering and Structural Dynamics 4 (1), 1–24.

Tseng, W.S., Penzien, J., 1975b. Seismic response of long multiple-span highway bridges. Earthquake Engineering and Structural Dynamics 4 (1), 25–48.

Wieser, J.D., Maragakis, E., Buckle, I.G., et al., 2012. Experimental evaluation of seismic pounding at seat-type abutments of horizontally curved bridges. In: Proceedings of 15th World Conference on Earthquake Engineering, Lisbon, 2012.

Williams, D., Godden, W., 1979. Seismic response of long curved bridge structures: experimental model studies. Earthquake Engineering and Structural Dynamics 7 (2), 107–128.

Wilson, E.L., Button, M., 1982. Three dimensional dynamic analysis for multi-component earthquake spectra. Earthquake Engineering and Structural Dynamics 10 (3), 471–476.

Yuan, W.C., Wang, Y.G., Yang, Y.M., 1996. Spatial seismic response analysis on the curved girder bridges. In: Proceedings of the 12th National Bridge Academic Conference, Shanghai, 1996.

Zhang, J.J., Lin, D.J., Hu, S.D., 1999. determine the most unfavorable input direction by seismic response spectrum method. World Earthquake Engineering 15 (4), 38–40.

Zhou, G.L., 2010. Canyon Topology Effects on Seismic Response of Multi-support Bridges (Ph.D thesis). China Earthquake Administration, Harbin.

Zhu, D.S., Liu, S.Z., Yu, L.S., 2002. Research on seismic response of curved girder bridges. China Journal of Highway and Transport 15 (3), 42–48.

Zhu, D.S., Yu, L.S., Liu, S.Z., 2000. The study of earthquake input principal direction for irregular bridges. Journal of Lanzhou Railway University 19 (6), 37–40.